Reiner Rivlin fluid in the case of mild stenosis ($\frac{\delta^*}{d_0} \ll 1$), subject to the additional conditions [4]

$$(i) \frac{Re \, \delta^* n^{\left(\frac{1}{n-1}\right)}}{b} \ll 1, \tag{11a}$$

$$(ii) \frac{d_0 n^{\left(\frac{1}{n-1}\right)}}{b} \sim O(1), \tag{11b}$$

can be written as

$$\frac{\partial u}{\partial r} + \frac{u}{r} + \frac{\partial w}{\partial z} = 0, \tag{12}$$

$$\frac{\partial p}{\partial r} = 0, \tag{13}$$

$$\frac{\partial p}{\partial z} = \frac{1}{r} \frac{\partial}{\partial r} \left[r \left(\left(\frac{\partial w}{\partial r} \right) + \lambda_1 \left(2 \frac{\partial w}{\partial r} \frac{\partial w}{\partial z} \right) \right) \right], \tag{14}$$

$$\frac{1}{r} \frac{\partial}{\partial r} \left(r \frac{\partial \theta}{\partial r} \right) + B_r \left(\left(\frac{\partial w}{\partial r} \right)^2 + \lambda_1 \left(2 \frac{\partial w}{\partial z} \right) \left(\frac{\partial w}{\partial r} \right)^2 \right) = 0, \tag{15}$$

$$\frac{1}{S_c} \left(\frac{1}{r} \frac{\partial}{\partial r} \left(r \frac{\partial \sigma}{\partial r} \right) \right) + S_r \left(\frac{1}{r} \frac{\partial}{\partial r} \left(r \frac{\partial \theta}{\partial r} \right) \right) = 0, \tag{16}$$

in which S_r is the Soret number, S_c Schmidt number, u_0 is the velocity averaged over the section of the tube of the width d_0 and σ is concentration.

The corresponding boundary conditions are

$$\frac{\partial w}{\partial r} = 0, \frac{\partial \theta}{\partial r} = 0, \frac{\partial \sigma}{\partial r} = 0 \text{ at } r = 0, \tag{17a}$$

$$w = 0, \theta = 0, \sigma = 0 \text{ at } r = h(z), \tag{17b}$$

where

$$h(z) = (1 + \xi z)[1 - \eta_1((z - \sigma) - (z - \sigma)^n)], \\ \sigma \le z \le \sigma + 1, \tag{18}$$

and

$$\eta_1 = \frac{\delta n^{\frac{n}{n-1}}}{(n-1)}, \quad \delta = \frac{\delta^*}{d_0}, \quad \sigma = \frac{a}{b}, \quad \xi' = \frac{\xi b}{d_0} \tag{19}$$

in which ($\xi = \tan \phi$), ϕ is called tappered angle and for converging tapering ($\phi < 0$), non-tapered artery ($\phi = 0$) and the diverging tappering ($\phi > 0$) (as shown in Fig. 2).

3 Solution of the problem

Since Eqs. 14 and 15 are non-linear equation so its exact solution is not possible. Therefore, we are seeking the perturbation solutions, for perturbation solution, we expand w, θ, σ, Q and p by taking λ_1 as perturbation parameter

$$w = w_0 + \lambda_1 w_1 + O(\lambda_1^2), \tag{20a}$$
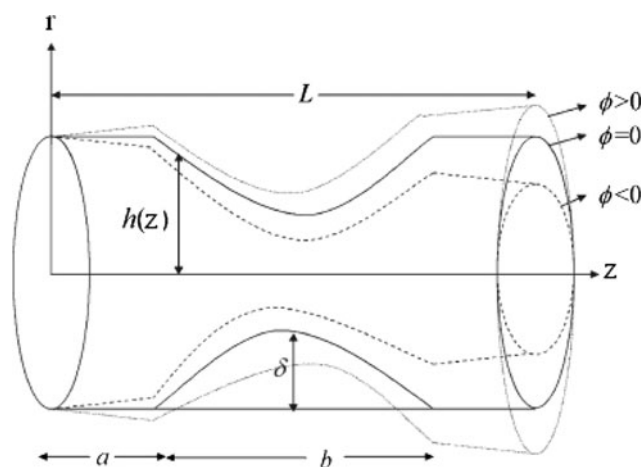
Fig. 2 Geometry of the axially stenosied tapered artery for different tapered angle

$$Q = Q_0 + \lambda_1 Q_1 + O(\lambda_1^2), \tag{20b}$$

$$p = p_0 + \lambda_1 p_1 + O(\lambda_1^2), \tag{20c}$$

$$\theta = \theta_0 + \lambda_1 \theta_1 + O(\lambda_1^2), \tag{20d}$$

$$\sigma = \sigma_0 + \lambda_1 \sigma_1 + O(\lambda_1^2). \tag{20e}$$

Making use of these above equations, the solutions for velocity, temperature and concentration, satisfying the boundary conditions take the form

$$w(r, z) = \left(\frac{r^2 - h^2}{4} \right) \frac{\partial p}{\partial z} + \lambda_1 \left(\frac{\partial p}{\partial z} \frac{\partial p'}{\partial z} \frac{1}{16} (r^4 - h^4) \right. \\ \left. -2h^2(r^2 - h^2) + \left(\frac{\partial p}{\partial z} \right)^2 \frac{hh'}{4} (r^2 - h^2) \right), \tag{21}$$

$$\theta(r, z) = -B_r \left(\left(\frac{r^4 - h^4}{64} \right) \left(\frac{dp}{dz} \right)^2 + \lambda_1 \left(a_8 \left(\frac{r^8 - h^8}{64} \right) \right. \right. \\ \left. \left. + a_9 \left(\frac{r^6 - h^6}{36} \right) + a_{10} \left(\frac{r^4 - h^4}{16} \right) \right) \right), \tag{22}$$

$$\sigma(r, z) = S_r S_c B_r \left(\left(\frac{r^4 - h^4}{64} \right) \left(\frac{dp}{dz} \right)^2 \right. \\ \left. + \lambda_1 \left(a_8 \left(\frac{r^8 - h^8}{64} \right) + a_9 \left(\frac{r^6 - h^6}{36} \right) \right. \right. \\ \left. \left. + a_{10} \left(\frac{r^4 - h^4}{16} \right) \right) \right). \tag{23}$$

We can defined the volume flow rate Q by

$$Q = \int_0^h rw \, dr, \tag{24}$$

Making use of the Eq. 21 into Eq. 24 and solving for dp/dz we get

$$\frac{dp}{dz} = -\frac{16Q}{h^4} + \lambda_1 \left(\frac{8Q}{3h^2} \left(-\frac{16Q}{h^4} \right)' - \frac{256Q^2 h'}{h^7} \right), \qquad (25)$$

The pressure drop ($\Delta p = p$ at $z = 0$ and $\Delta p = -p$ at $z = L$) across the stenosis between the section $z = 0$ and $z = L$ can be obtain from (25) as done by [4]

$$\Delta p = \int_0^L \left(-\frac{dp}{dz} \right) dz, \qquad (26)$$

3.1 Resistance impedance

The expression resistance impedance is defined as

$$\tilde{\lambda} = \frac{\Delta p}{Q}$$
$$= \left\{ \int_0^a \int F(z)|_{h=1} dz + \int_a^{a+b} \int F(z) dz + \int_{a+b}^L \int F(z)|_{h=1} dz \right\}, \qquad (27)$$

where

$$F(z) = \frac{16}{h^4} + \lambda_1 \left(-\frac{8}{3h^2} \left(-\frac{16Q}{h^4} \right)' + \frac{256Qh'}{h^7} \right).$$

Eq. (27) in simplified form can be written as

$$\tilde{\lambda} = \left\{ (L - b) \left(16 + \lambda_1 \left(-\frac{8}{3}(-16Q)' + 256Qh' \right) \right) + \int_a^{a+b} \int F(z) dz \right\}. \qquad (28)$$

3.2 Expression for the wall shear stress

The nonzero dimensionless shear stress is given by

$$\tilde{\tau}_{rz} = \left(2 \left(\frac{\partial w}{\partial r} \right) + \lambda_1 \left(2 \frac{\partial w}{\partial r} \frac{\partial w}{\partial z} \right) \right), \qquad (29)$$

From Eq. (29) we can find the expression for wall shear stress by

$$\tilde{\tau}_{rz} = \left(2 \left(\frac{\partial w}{\partial r} \right) + \lambda_1 \left(2 \frac{\partial w}{\partial r} \frac{\partial w}{\partial z} \right) \right) \Bigg|_{r=h}, \qquad (30)$$

With the help of Eq. 21, Eq. 30 can be written as

$$\tilde{\tau}_{rz} = a_{11} r^7 + a_{12} r^5 + a_{13} r^3 + a_{14} r + a_{15}, \qquad (31)$$

We can note that the shearing stress at the stenosis throat i.e the wall shear at the maximum height of the stenosis located at $z = \frac{a}{b} + \frac{1}{n^{\frac{n}{n-1}}}$ i.e $\tilde{\tau}_s = \tilde{\tau}_{rz}|_{h=1-\delta}$ is

$$\tilde{\tau}_s = a_{11} r^7 + a_{12} r^5 + a_{13} r^3 + a_{14} r + a_{15}|_{h=1-\delta}. \qquad (32)$$

where $a_1 - a_{15}$ are defined in appendix.

We can find the final expression for the dimensionless resistance to λ, wall shear stress τ_{rz} and the shearing stress at the throat τ_s are defined as

$$\lambda = \frac{1}{3} \left\{ \left(1 - \frac{b}{L} \right) \left(16 + \lambda_1 \left(-\frac{8}{3}(-16Q)' + 256Qh' \right) \right) + \frac{1}{L} \int_a^{a+b} \int F(z) dz \right\}, \qquad (33)$$

$$\tau_{rz} = \frac{1}{4Q} (a_{11} r^7 + a_{12} r^5 + a_{13} r^3 + a_{14} r + a_{15}), \qquad (34)$$

$$\tau_s = \frac{1}{4Q} (a_{11} r^7 + a_{12} r^5 + a_{13} r^3 + a_{14} r + a_{15}|_{h=1-\delta}), \qquad (35)$$

where

$$\lambda = \frac{\tilde{\lambda}}{\lambda_0}, \quad \tau_{rz} = \frac{\tilde{\tau}_{rz}}{\tau_0}, \quad \tau_s = \frac{\tilde{\tau}_s}{\tau_0}, \quad \lambda_0 = 3L, \quad \tau_0 = 4Q.$$

4 Numerical results and discussion

To observe the quantitative effects of the Reiner Rivlin fluid parameter λ_1, the stenosis shape n and maximum height of the stenosis δ for converging tapering, diverging tapering and non-tapered arteries for Reiner Rivlin fluid. We have made Figs. 3, 4, 5, 6, 7, 8, 9, 10, 11 and 12. The variation of axial velocity for λ_1, n, and δ for the case of a converging tapering, diverging tapering and non-tapered arteries are displayed in Figs. 3, 4 and 5. We observed that with an increase in λ_1, n and δ, velocity profile decreases.
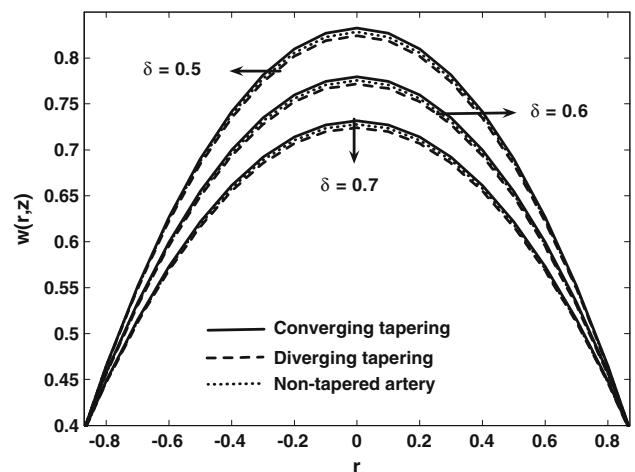
Fig. 3 Variation of velocity profile for $Q = 0.3$, $\sigma = 0.0$, $z = 0.5$, $n = 2$, $\lambda_1 = 0.3$
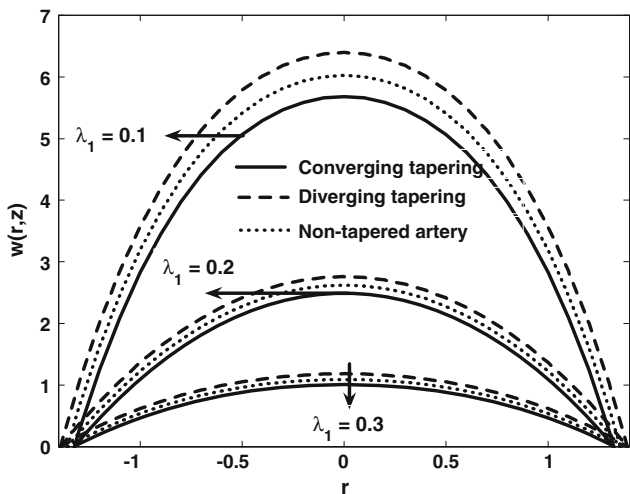
Fig. 4 Variation of velocity profile for $Q = 0.3$, $\sigma = 0.0$, $z = 0.5$, $n = 2$, $\lambda_1 = 0.3$
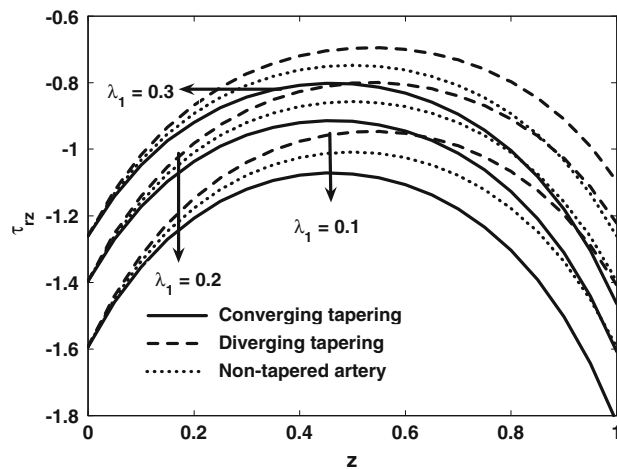
Fig. 7 Variation of wall shear stress for $Q = 0.3$, $n = 2$, $\sigma = 0.0$, $\delta = 0.3$
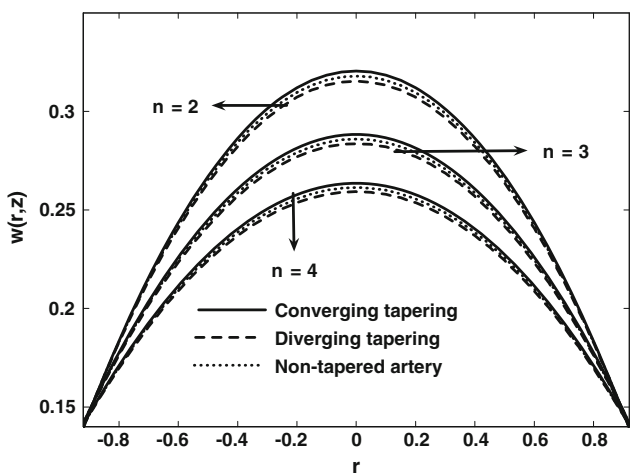
Fig. 5 Variation of velocity profile for $Q = 0.3$, $\sigma = 0.0$, $z = 0.5$, $\delta = 0.2$, $\lambda_1 = 0.3$
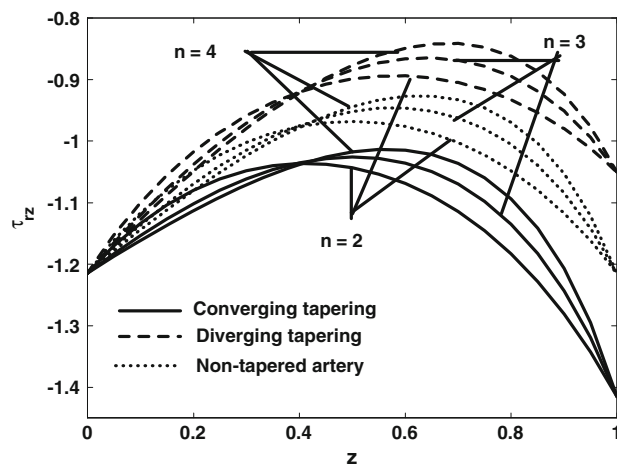
Fig. 8 Variation of wall shear stress for $Q = 0.3$, $\lambda_1 = 0.2$, $\sigma = 0.0$, $\delta = 0.3$
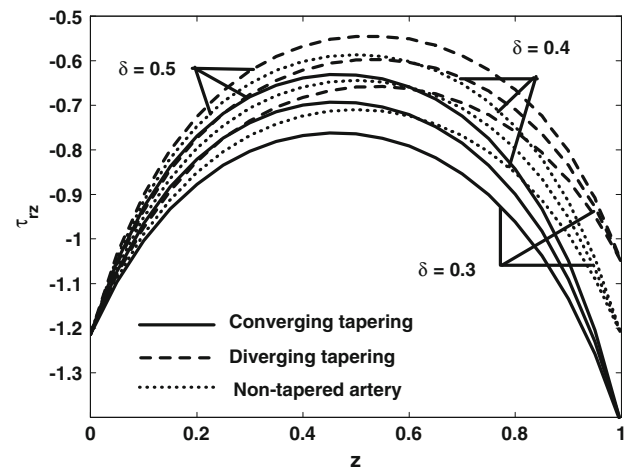
Fig. 6 Variation of wall shear stress for $Q = 0.3$, $n = 2$, $\sigma = 0.0$, $\lambda_1 = 0.3$
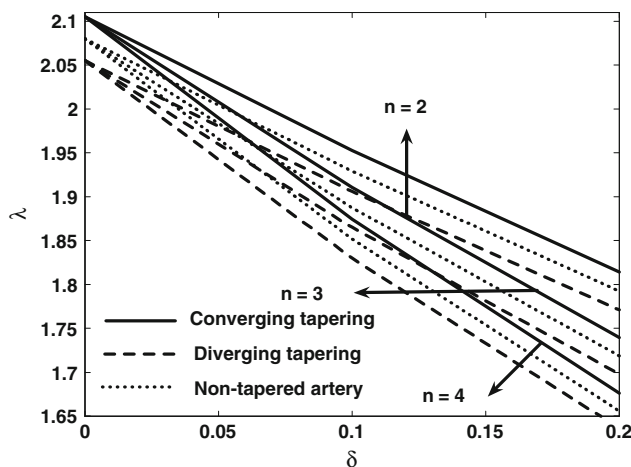
Fig. 9 Variation of resistance for $Q = 0.3$, $L = 1$, $\sigma = 0.0$, $b = 0.6$, $\lambda_1 = 0.3$, $z = 0.5$
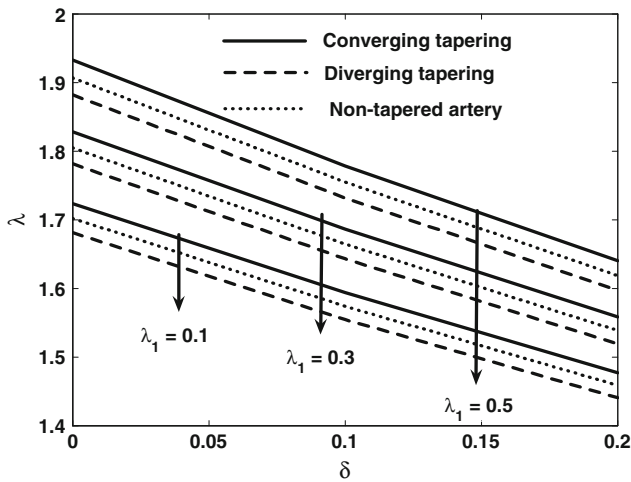
Fig. 10 Variation of resistance for $Q = 0.3$, $L = 1$, $\sigma = 0.0$, $b = 0.6$, $n = 2$, $z = 0.5$
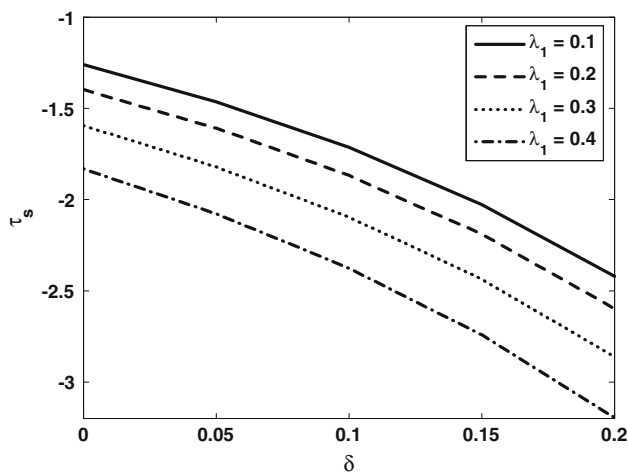
Fig. 11 Variation of shear stress at the stenosis throat for $Q = 0.3$
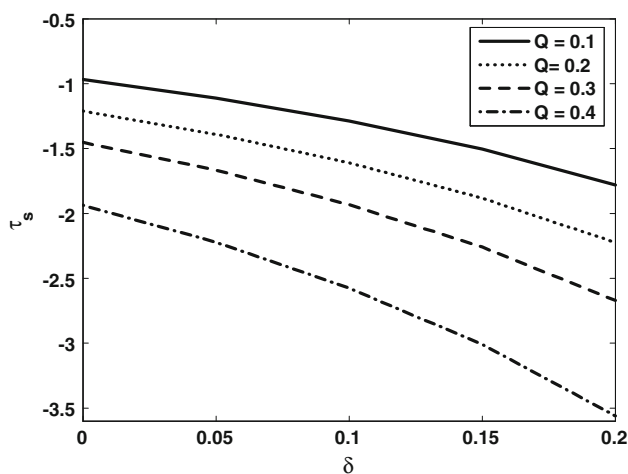
Fig. 12 Variation of shear stress at the stenosis throat for $\lambda_1 = 0.3$

It is also seen that for the case of converging tapering velocity gives larger values as compared to the case of diverging tapering and non-tapered arteries. Figures 6, 7 and (8 show how the converging tapering, diverging tapering and non-tapered arteries influence on the wall shear stress τ_{rz}. It is observed that with an increase in λ_1, n, and δ shear stress increases, the stress yield diverging tapering with tapered angle $\phi > 0$, converging tapering with tapered angle $\phi < 0$ and non-tapered artery with tapered angle $\phi = 0$. In Figs. 9 and 10 we notice that the impedance resistance increases for converging tapering, diverging tapering and non-tapered arteries when we increase λ_1, while decreases when we increase n. We also observed that resistive impedance in a diverging tapering appear to be smaller than those in converging tapering because the flow rate is higher in the former than that in the latter, as anticipated and impedance resistance attains its maximum values in the symmetric stenosis case ($n = 2$). Finally Figs. 11 and 12 are prepared to see the variation of the shearing stress at the stenosis throat τ_s with δ. It is analyzed that shearing stress at the stenosis throat decreases with an increase in Q and λ_1. Figures 13 and 14 show the variation of temperature profile for different values of Brickmann number B_r and Reiner Rivlin fluid parameter λ_1. It is observed that with an increase in Brickmann number B_r, temperature profile decreases while increases with an increase in Reiner Rivlin fluid parameter λ_1 and temperature profile gives the large values for converging tapering as compared to the diverging and non-tapered artery. Figures 15, 16 and 17 are prepared to see the variation of concentration profile for Brickmann number B_r, Reiner Rivlin fluid parameter λ_1 and Soret number S_r. It is
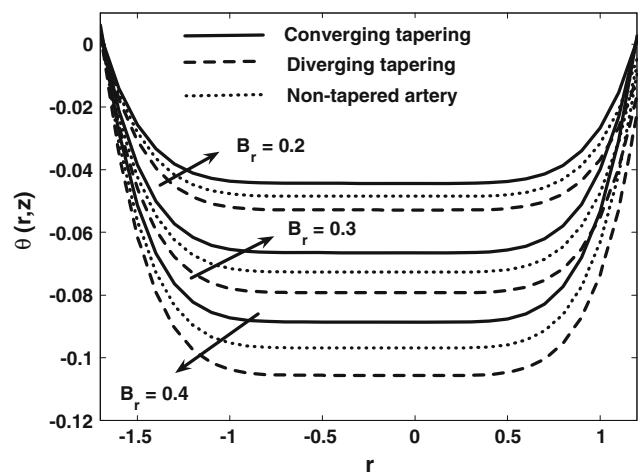
Fig. 13 Variation of temperature profile for $Q = 0.3$, $\sigma = 0.0$, $z = 0.5$, $n = 2$, $\lambda_1 = 0.3$. $\delta = 0.3$